New Physics Opportunities in the Boosted Di-Higgs-Boson Plus Missing Transverse Energy Signature

Zhaofeng Kang,[1,*] P. Ko,[1,†] and Jinmian Li[2,‡]
[1]School of Physics, Korea Institute for Advanced Study, Seoul 130-722, Korea
[2]ARC Centre of Excellence for Particle Physics at the Terascale, Department of Physics, University of Adelaide, Adelaide, South Australia 5005, Australia

(Received 4 June 2015; revised manuscript received 19 November 2015; published 1 April 2016)

The Higgs field in the standard model may couple to new physics sectors related to dark matter and/or massive neutrinos. In this Letter we propose a novel signature, the boosted di-Higgs-boson plus $\not{E}_T$ (which is either a dark matter or neutrino), to probe those new physics sectors. In a large class of models, in particular, the supersymmetric standard models and low scale seesaw mechanisms, this signature can play a key role. The signature has a clear background, and at the $\sqrt{s} = 14$ TeV high luminosity LHC, we can probe it with a production rate as low as ~0.1 fb. We apply it to benchmark models, supersymmetry in the bino-Higgsino limit, the canonical seesaw model, and the little Higgs model, finding that the masses of the Higgsino, right-handed neutrino, and heavy vector boson can be probed up to ~500, 650, and 900 GeV, respectively.

DOI: 10.1103/PhysRevLett.116.131801

New physics below the iceberg discovery of the Higgs boson at the Large Hadron Collider (LHC) [1] completes the standard model (SM). At the same time, however, it opens a new era for particle physics: this new resonance might be just a small tip of a big iceberg, and below it could hide a mystery of a new world. Looking around this small tip, we may find clues for new physics. Actually, we do have convincing arguments to support this belief from several motivations for new physics beyond the SM (BSM).

The most common theoretical argument for new physics is from the notorious gauge hierarchy problem caused by the quadratic divergence of the $(\text{Higgs mass})^2$ parameter. Solutions to this problem introduce new particles coupled to the SM Higgs-boson field. For instance, in the supersymmetric SMs (SSMs) the Higgs-boson doublet H_u (along with H_d by virtue of anomaly cancellation) participates in quite a few interactions. The second argument for new physics is from dark matter (DM), whose interactions with the visible sector may be through the SM Higgs boson h (Higgs portal DM). Last but not the least, neutrinos in the renormalizable SM are massless, in conflict with the observation. Mechanisms, such as various seesaw mechanisms, to generate neutrino masses may again introduce new couplings to h. It is well expected that these new interactions of h could contribute to the production of h (plus something else) at the LHC. In this Letter we will concentrate on the di-Higgs-boson production, which is common in these mentioned BSM contexts, has a bright prospect at the LHC, and, moreover, provides a new angle on di-Higgs-boson physics.

BSM with boosted di-Higgs bosons plus $\not{E}_T$.—The di-Higgs-boson search is one of the focuses in the upcoming LHC run, aiming at examining the Higgs-boson potential [2,3]. On the other hand, on top of the di-Higgs boson, a large class of BSM models can produce associated objects X; e.g., X is a missing particle at the LHC, such as DM or neutrino. Moreover, both Higgs bosons may be boosted if they are produced from heavy particle decay. These additional features could greatly enhance the di-Higgs-boson searches at a hadronic collider. In the following, we select two well-known BSM models where X is a DM and neutrino, respectively.

The first example is the neutralino sector of the minimal SSM (MSSM) with bino-Higgsino accessible at the LHC only, $\psi = (\tilde{B}, \tilde{H}_d^0, \tilde{H}_u^0)$. [The gravitino-Higgsino system with very light (say, ~keV) gravitino from the low scale supersymmetry-breaking models fit this scenario better. We leave it for a future study.] Since we are interested in the boosted di-Higgs boson, we assume such a mass hierarchy: Higgsinos $\tilde{H}_{u,d}^0$ (with mass $\mu \sim 500$ GeV) are much heavier than bino $\tilde{B}$ (with mass $\lesssim 100$ GeV). The mass eigenstates $\chi_{1,2,3}$, respectively, having masses $M_{1,2,3}$ in ascending order, are related to ψ via $\psi_i = Z_\psi^{ij}\chi_j$. χ_2 and χ_3 are Higgsino-like, constituting a pseudo-Dirac fermion pair with masse splitting of a few GeV; χ_1 is treated as massless for the moment. Electroweak gauge interactions of these particles are described by

$$\mathcal{L}_\chi = \frac{g_2}{2}\tan\theta_w \bar{\chi}_i a_{ij}^h \chi_j h + \frac{g_2}{4\cos\theta_w}\bar{\chi}_i a_{ij}^z \gamma_5 \gamma_\mu \chi_j Z^\mu, \quad (1)$$

with θ_w the Weinberg angle and $a_{ij}^h = Z_\psi^{2j} Z_\psi^{1i}$, $a_{ij}^z = Z_\psi^{3i} Z_\psi^{3j} - Z_\psi^{2i} Z_\psi^{2j}$. We have assumed CP invariance and an exact decoupling between two Higgs doublets. Note that the diagonal couplings a_{ii}^z are suppressed by the small mass splitting between M_2 and M_3.

The interesting signature is produced along the chain $pp \to Z^* \to \chi_2(\to \chi_1 h)\chi_3(\to \chi_1 h)$. In the high energy limit $M_{2,3}^2 - M_1^2 \gg m_Z^2$, we can apply the Goldstone equivalence theorem and obtain the following equations for decay branching ratios of $\chi_{2,3}$ (we refer to Ref. [4] for relevant discussions on this point):

$$\frac{\Gamma(\chi_2 \to h+\chi_1)}{\Gamma(\chi_3 \to Z+\chi_1)} \approx \frac{\Gamma(\chi_2 \to Z+\chi_1)}{\Gamma(\chi_3 \to h+\chi_1)}. \tag{2}$$

This theorem will be used frequently in this Letter. In order to approach the maximal branching ratio of the di-Higgs-boson channel, $\Gamma(\chi_i \to h+\chi_1) \approx \Gamma(\chi_i \to Z+\chi_1) = 50\%$ is favored. And it holds when the Higgs-boson sector gives a large $\tan\beta$ limit and, moreover, $|\mu| \approx |M_{2,3}| \gg M_1$. In this limit the cross section of di-Higgs-boson plus $\not{E}_T$ can reach 1.2 fb for 500 GeV Higgsinos.

The second example is the heavy right-handed neutrino (RHN) N in the type-I seesaw mechanism implemented in the local $B-L$ model [5]. The minimal model is described by the following Lagrangian:

$$-\mathcal{L}_N = g_{B-L}\bar{N}\gamma_\mu P_R N Z_{B-L}^\mu + y_N \bar{\ell}\,\tilde{H}\,P_R N + \frac{1}{2}\lambda_N \Phi \bar{N}^c N + \text{H.c.} + V(\Phi, H), \tag{3}$$

where we consider only one family of RHN for simplicity. N carries one unit of $B-L$ charge and gains Majorana mass from the coupling to the $B-L$ Higgs-boson field Φ, which develops vacuum expectation value v_ϕ from the potential $V(\Phi, H)$ and breaks $U(1)_{B-L}$ at the TeV scale. The term $|\Phi|^2|H|^2$ in $V(\Phi, H)$ mixes Φ and H^0, the neutral component of SM doublet H, leading to two Higgs bosons in the mass eigensate:

$$h = \cos\theta H_R^0 + \sin\theta \Phi_R, \quad \phi = -\sin\theta H_R^0 + \cos\theta \Phi_R. \tag{4}$$

We have decomposed $\Phi = (v_\phi + \Phi_R + i\Phi_I)/\sqrt{2}$ similarly for H^0. The current data tell us that h is quite SM-like, and the measured Higgs-boson signal strength imposes an upper bound on the mixng angle $\sin\theta \lesssim 0.34$ at the 95% C.L. [6]. For such a small mixing angle, the SM-like Higgs-boson mass squared can be approximated as

$$m_h^2 \approx \lambda_h v^2 - \sin^2\theta m_\phi^2, \tag{5}$$

where λ_h is the usual Higgs-boson quartic self-coupling. Let us mention that the heavier ϕ and the larger θ are good for solving the metastability problem of the Higgs-boson potential near the Plank scale, which is attributed to the relatively small $\lambda_h = \lambda_{\rm SM} \approx 0.26$. For example, for $m_\phi = 1.0$ TeV and $\sin\theta = 0.3$, we now need $\lambda_h \approx 1.7$. Note that such discussions can be easily generalized to other models.

The heavy N can be abundantly pair produced via the resonance Z_{B-L}/ϕ: $pp \to Z_{B-L}/\phi \to NN$. The Z_{B-L} channel is suppressed by the small branching ratio $\text{Br}(Z_{B-L} \to NN) \approx 3\%$. In addition to that, it is strongly constrained by the dilepton resonance search $pp \to Z_{B-L} \to \bar{\ell}\ell$ at the LHC [7]. The ϕ channel is due to the gluon-gluon fusion production of ϕ, described by the usual dimension-five operator for $\phi \to gg$:

$$\frac{1}{4} C_{gg\phi} G_{\mu\nu}^a G^{a\mu\nu} \frac{\phi}{v}, \tag{6}$$

with $C_{gg\phi} = -\sin\theta\alpha_s/2\pi$. However, this effective description becomes invalid when m_ϕ is much heavier than the top quark mass. Therefore, in the actual LHC analysis, we will utilize the results from the CERN Yellow Report [8], which takes into account the finite top quark mass effect. For $\lambda_N \sim 1$, one can naturally expect $\text{Br}(\phi \to NN) \sim 100\%$. The RHN pair is followed by the decay $N \to \nu_L h$, with ν_L the active neutrino, giving rise to the boosted di-Higgs-boson plus $\not{E}_T$ signature. Because RHN is heavy, the branching ratios satisfy the relations [5,9]

$$\Gamma(N \to \nu_L h) \approx \Gamma(N \to \nu_L Z) = \frac{1}{2}\Gamma(N \to \ell W), \tag{7}$$

which again follows from the equivalence theorem. For $M_N = 0.5$ TeV, one can reach a signal cross section I.5 fb given that m_ϕ is about 1 TeV.

Comments are in order. The conventional single RHN (below the weak scale) production counts on sizable mixings between the sterile and active neutrinos [10,11], which would be extremely small in generic cases. But RHN probably has gauge and/or Yukawa couplings, e.g., in the local $B-L$ models, and thus the pair production of heavy RHN is hopeful at 14 TeV LHC or other future colliders. In particular, to our knowledge, using a scalar resonance is novel in RHN production and may offer the unique chance to probe a type-I seesaw mechanism.

Simplified models for $2h + \not{E}_T$.—There are many other well-motivated BSM models that can produce this signature; see an incomplete collection in the Supplemental Material [12]. Therefore, before we head to the detailed collider study, this would be the right place to develop simplified models which could be used for a more general study of this signature.

Two classes of models are of interest. Let us start with the first class, where the missing particle is DM, or, more widely, a neutral particle stable at the collider time scale. The dark sector is supposed to consist of several dark states; we will use this term to genetically refer to particles undiscovered. And we will consider two dark states for concreteness. Then their interactions with the Higgs boson would take the following forms:

$$\lambda_f h\chi_1\chi_2, \qquad \mu_s h S_1 S_2, \qquad g_Z h Z_2^\mu (Z_1)_\mu. \tag{8}$$

(χ_1, S_1, Z_1) is a (Majorana fermion, real scalar, vector boson) DM with negligible mass; the heavy dark state χ_2,

S_2, and Z_2 are in the sub-TeV mass region. Similarly, the second class with a neutrino as the missing particle can be built. The RHN-like heavy state N couples to the neutrino and Higgs boson via the effective operator

$$\lambda_\nu h N \nu_L. \tag{9}$$

With these, the event topology boosted $2h + \not{E}_T$ is generated through pair production of heavy dark states which decay into DM or neutrino plus Higgs bosons.

In the simplified models we do not specify the production mechanism for the father particle F, such as χ_2, since it is fairly model dependent. We can consider three possibilities for F productions. First, the father particle F itself, such as the Higgsino, has electroweak interactions so that the F pair can be produced via Drell-Yan processes. This mechanism does not involve extra particles and couplings. Second, in the presence of a new particle Y coupling to light quarks q as $\sim qYF$ (just schematically), F can be pair produced via exchanging Y in the t channel. In the Supplemental Material [12], the vector F pair production in the little Higgs-boson model is discussed in this way. Last but not the least, if Y has interactions like $\sim Yqq/GG + YFF$, then the F pair can be resonantly produced. But as mentioned before, this contribution will be stringently restricted if Y also couples significantly to leptons. The latter two possibilities may provide more effective production mechanisms than the first one, provided that the mass and couplings of Y (to quarks and F) are proper. In the following studies, a proper production mechanism for the F pair will be assumed.

Boosted $2h + \not{E}_T$ at the 14 TeV LHC.—The hadronic $4b$ mode is dominant in the di-Higgs-boson decay, and may rise above the huge QCD backgrounds (BGs) in the boosted region. For example, Lima *et al.* show that with the help of the boosted di-Higgs-boson channel one can finally reach $1.2\lambda_{\rm SM}$ at the 14 TeV high luminosity LHC [20]. (The ATLAS search on a data set of 8 TeV 19.5 fb^{-1} shows that the current search sensitivity to the boosted di-Higgs-boson channel is around an order of magnitude above the SM di-Higgs-boson production rate [21], without using the substructure technique.) This channel was believed to not be promising [22,23] outside of the boosted Higgs-boson region. In some new physics scenarios, where the di-Higgs boson is produced from a heavy resonance decay, this channel is even more remarkable [24–26]. Other related studies involving boosted (maybe extra) Higgs boson(s) are also motivated in various contexts [25, 27–30]. In our signature, the (highly) boosted di-Higgs boson is further strengthened by a large missing energy that could lead to the much earlier discovery of $2h + \not{E}_T$ than the previous signatures without $\not{E}_T$. (The CMS Collaboration searched for this signature without using boosted Higgs-boson tagging [31]. They required that all $4b$'s have to be resolved).

The BGs of $2h + \not{E}_T$ are similar to those of the di-Higgs-boson signature: the irreducible BGs (dominated by QCD $4b$ and $Zb\bar{b}$) and the reducible BGs (dominated by the semileptonic $t\bar{t}$ pair); $4j$ with $j = g, u, d, s, c$ can be mistagged as $4b$, but the cross section is $\lesssim 10^{-3}\sigma(4b)$, and thus negligible. In the irreducible BGs, $\not{E}_T$ is due to the limited detector resolution, and the distribution of $\not{E}_T$ depends on the detector setup: e.g., at 7 TeV LHC it respects a Gaussian distribution with the central value $\sim 0.5\sqrt{\sum p_T}$ GeV [32]. While in the semileptonic $t\bar{t}$ BG, light flavor jets can be mistagged as b jets and at the same time the leptons may be missed owing to the limited lepton tagging efficiencies (especially for τ); besides, leptons will also be missed if the leptons go outside the kinematic region, i.e.,$p_T(l) > 10$ GeV and $|\eta| < 2.5$, or they are not isolated, i.e., the scalar p_T sum of particles in the vicinity ($\Delta R < 0.5$) of the lepton is greater than $10\% \times p_T(l)$. MadGraph5_aMC@NLO [33] is used to calculate the leading order (LO) cross sections for $4b$ (861 pb) and $Zb\bar{b}$ (109 pb at next-to-leading order (NLO) after multiplying a constant K factor 1.4 [34]); the bottom quarks in these BGs are required to have $p_T(b) > 20$ GeV, $|\eta(b)| < 2.5$, and $\Delta R(b,b) > 0.4$. The next-to-next-to-leading order (NNLO) cross section of the semileptonic $t\bar{t}$ including all lepton flavors can be found in Ref. [35], 382 pb; no cuts are imposed on the top decay products.

We take heavy RHN pair production via the ϕ resonance as the representative signal process, setting $m_\phi = 2M_N + 30$ GeV and $\text{Br}(N \to h\nu_L) = 1$. FEYNRULES [36] is used for generating the Universal FeynRules Output (UFO) model files of the model [37]. The signal (and BGs) events are generated by MadGraph5_aMC@NLO, and passed to PYTHIA6 [38] for SM particle decay, parton showering, and hadronization. The detector effects are simulated with DELPHES3 [39], where we choose the default ATLAS detector setup. The b-tagging efficiency is set to 0.7 with mis-b-tagging rates for c- and light-flavored jets assumed to be 0.1 and 0.015 [40], respectively. Then, the particle flow information from DELPHES3 is analyzed using FASTJET [41].

Comments on the generalization of the above representative model are in order. First, the invisible particle is assumed to be massless. However, our results can be generalized to the massive invisible particle case ($\not{E}_T$ refers to the measurable $\not{p}_T$ in this case), because the variables in our analysis actually are merely sensitive to the mass difference between the invisible particle and the father particle. Second, we have chosen the Yukawa coupling of ϕ such that the narrow width approximation holds ($\Gamma_\phi \lesssim 0.1 m_\phi$); moreover, $m_\phi - 2M_N$ is small. So, it is justified to conclude that the kinematic properties of the RHN pair produced here are similar to those of the F pair, which is produced in other ways through an off-shell s-channel mediator or a t-channel mediator.

In selecting the signal events, lepton veto is imposed first. Next, the Cambridge-Aachen algorithm [42] with an

TABLE I. The selection efficiency S and cross sections of BGs after applying Higgs tagging, which takes $m_{\rm Higgs} \in [85, 160]$ GeV and $R_{\rm fat} = R_{\rm fat}^{\rm max}$.

M_N (GeV)	$R_{\rm fat}^{\rm max}$	S	$t\bar{t}$ (fb)	$Zb\bar{b}$ (fb)	QCD (fb)
200	2.0	2.1%	5.2	13.9	591.8
300	1.8	2.5%	3.9	9.2	399.4
400	1.6	3.2%	2.4	5.6	241.7
500	1.6	3.9%	2.4	5.6	241.7
700	1.4	5.4%	1.3	2.9	117.1
1000	1.0	6.8%	0.46	0.41	14.5
2000	0.8	8.8%	0.19	0.1	3.2

appropriate cone size $R_{\rm fat}$ is used to recluster fat jets. Then the BDRS algorithm [43] is applied to resolve their substructure. More concretely, a Higgs-boson jet candidate during the declustering should have large mass drop $\mu = m_{j_1}/m_j < 0.67$, and not too asymmetric mass splitting $y = [\min(p_{T,j_1}^2, p_{T,j_2}^2)/m_j^2]\Delta R_{j_1,j_2}^2 > 0.09$. After filtering, the three hardest subjets inside the fat jet, which are reconstructed by the anti-kt algorithm with $R_{\rm filt} = \min(0.3, R_{b\bar{b}}/2)$, are identified as the ingredients of the Higgs jet candidate; also, the two leading subjets are required to be b tagged.

The separation angle between b and $\bar{b}$ from Higgs decay, namely, the Higgs jet cone size, depends on the energy of the Higgs boson. For each RHN mass M_N, we scan $R_{\rm fat} \in [0.5, 3]$ with step size 0.1 and find $R_{\rm fat}^{\rm max}$, which retains most of the signal events whose leading two fat jets pass the BDRS Higgs-tagging criteria and the cut $m_{\rm Higgs} \in [85, 160]$ GeV (a more refined mass interval for a given M_N is given in Table II). In Table I we show the options of $R_{\rm fat}^{\rm max}$ for different values of M_N. The fraction of retained signal events (selection efficiency) and cross sections of BGs after Higgs tagging are also displayed. As expected, a smaller $R_{\rm fat}^{\rm max}$ should be adopted for a heavier N. It then greatly reduces the probability that two close QCD jets mimic the Higgs jet, thus suppressing BGs (especially the QCD BG from $4b$'s).

There are some other powerful discriminators in our analysis, such as $\not{E}_T$ and the reconstructed two Higgs boson masses. Requiring $\not{E}_T \gtrsim 100$ GeV after Higgs-boson tagging leaves the semileptonic $t\bar{t}$ as the dominant BG. In addition, since we consider pair production of heavy particles, the M_{T_2} variable [44], which reflects mass difference between the father particle and its invisible daughter, is quite useful. According to these variables, we design four signal regions (SR) which are suitable for different M_N; see Table II where the name of the SR is indicated by the RHN mass. The cuts of each SR are optimized with respect to the corresponding benchmark point. Note that SR500 will be used for M_N above 500 GeV because its BGs already become negligible.

TABLE II. Optimized cuts for the four signal regions.

Signal region	SR200	SR300	SR400	SR500
Selection cuts	Lepton veto and tau veto		Two Higgs tagged jets	
$\not{E}_T$/ GeV	> 100	> 100	> 200	> 300
m_{h_1}/ GeV	[90,150]	[90,150]	[90,150]	[90,150]
m_{h_2}/ GeV	[80,140]	[70,150]	[80,140]	[80,140]
$M_{T_2}(h_1, h_2)$	> 130	> 170	> 215	> 300

How far can we reach?—For a given RHN mass, the signal cross section that provides at least 3σ significance, i.e., $S/\sqrt{S+B} \geq 3$, is

$$\sigma_S \geq \frac{1}{\epsilon_S \mathcal{L}} \frac{9 + \sqrt{81 + 36 \times \sigma_B \epsilon_B \mathcal{L}}}{2}, \qquad (10)$$

where $\mathcal{L}$ is the integrated luminosity and $\epsilon_{S,B}$ are cut efficiencies for the signal and BGs, respectively. In Fig. 1 we show the reach limit of our representative signal process in the light green shaded region. One can see that the production rate as low as $\mathcal{O}(0.1)$ fb can be reached for $M_N > 500$ GeV.

Now we explain the above model-independent reach in several benchmark models, where the kinematic properties of the father particle (F) pair are similar to those of the RHN pair in the representative signal process. They are (I) the neutrino system in the type-I seesaw that presents a scalar resonance ϕ with a large mass $m_\phi \gtrsim 2M_N$ [for such heavy ϕ, its production rate is obtained from Ref. [8] rather than Eq. (6)], the mixing angle (converting the signal reach to the limit on the mixing angle for ϕ, we get $\sin\theta \gtrsim 0.23$ for m_ϕ around 800 GeV, but it can be improved much at the 100 TeV collider [45]) $\sin\theta = 0.3$, and $\mathrm{Br}(\phi \to NN) = 1$; (II) the bino-Higgsino system in MSSM with $\mathrm{Br}(\tilde{H}_{u,d}^0 \to \tilde{B}h) = 50\%$; (III) the sneutrino system $\tilde{\nu}_L - \tilde{N}$ in the supersymmetric seesaw [46] with the left-handed

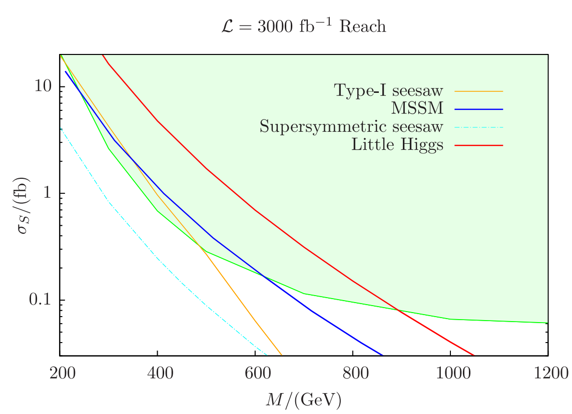

FIG. 1. Based on the representative signal process, the shaded region can be probed with 3σ significance at 14 TeV 3000 fb^{-1} LHC. We display the cross sections of di-Higgs + $\not{E}_T$ in four models: (I) seesaw (orange line), (II) MSSM (blue line), (III) supersymmetric seesaw (cyan line), and (IV) little Higgs boson (red line) models.

sneutrino $\tilde{\nu}_L$ produced via the Drell-Yan process and $\mathrm{Br}(\tilde{\nu}_L \to \tilde{N} + h) = 50\%$; (IV) the massive vector boson system $Z_H - A_H$ in the little Higgs-boson model [47,48] with Z_H produced by the t-channel exchange of a quark partner and $\mathrm{Br}(Z_H \to A_H + h) = 100\%$. We put the details of the latter two models in the Supplemental Material [12]. The 3σ discovery lines are labeled in Fig. 1. We observe that (RHN, Higgsinos, Z_H) with mass up to $\sim(0.50, 0.65, 0.9)$ TeV can be probed at the 3σ level, whereas the sneutrino case can hardly be probed. Note that the invisible particle is assumed to be massless, and the violation of this assumption will lead to a shift of these curves toward the left, roughly by the invisible particle mass.

Conclusion.—In light of a large class of BSM models, we propose a noble signature, namely, the boosted di-Higgs-boson plus $\not{E}_T$ to probe new physics. Good prospects of models like MSSM, type-I seesaw, and the little Higgs boson are demonstrated, finding that masses of Higgsino, right-handed neutrino, and heavy vector bosons can be probed up to ∼500, 650, and 900 GeV, respectively.

This work is supported in part by National Research Foundation of Korea (NRF) Research Grant No. NRF-2015R1A2A1A05001869, and by the NRF grant funded by the Korea government (MSIP) (No. 2009-0083526) through Korea Neutrino Research Center at Seoul National University (P. K.).

*zhaofengkang@gmail.com
†pko@kias.re.kr
‡phyljm@gmail.com

[1] G. Aad *et al.* (ATLAS Collaboration), Observation of a new particle in the search for the Standard Model Higgs boson with the ATLAS detector at the LHC, Phys. Lett. B **716**, 1 (2012); S. Chatrchyan *et al.* (CMS Collaboration), Observation of a new boson at a mass of 125 GeV with the CMS experiment at the LHC, Phys. Lett. B **716**, 30 (2012).

[2] R. S. Gupta, H. Rzehak, and J. D. Wells, How well do we need to measure the Higgs boson mass and self-coupling?, Phys. Rev. D **88**, 055024 (2013).

[3] A. Papaefstathiou, L. L. Yang, and J. Zurita, Higgs boson pair production at the LHC in the $b\bar{b}W^+W^-$ channel, Phys. Rev. D **87**, 011301 (2013); M. J. Dolan, C. Englert, and M. Spannowsky, New physics in LHC Higgs boson pair production, Phys. Rev. D **87**, 055002 (2013); F. Goertz, A. Papaefstathiou, L. L. Yang, and J. Zurita, Higgs Boson self-coupling measurements using ratios of cross sections, J. High Energy Phys. 06 (2013) 016; J. Cao, Z. Heng, L. Shang, P. Wan, and J. M. Yang, Pair production of a 125 GeV Higgs boson in MSSM and NMSSM at the LHC, J. High Energy Phys. 04 (2013) 134; U. Ellwanger, Higgs pair production in the NMSSM at the LHC, J. High Energy Phys. 08 (2013) 077; J. Liu, X. P. Wang, and S. h. Zhu, Discovering extra Higgs boson via pair production of the SM-like Higgs bosons, arXiv:1310.3634; P. Maierhöfer and A. Papaefstathiou, Higgs boson pair production merged to one jet, J. High Energy Phys. 03 (2014) 126; C. R. Chen and I. Low, Double take on new physics in double Higgs boson production, Phys. Rev. D **90**, 013018 (2014); T. Liu and H. Zhang, Measuring Di-Higgs physics via the $t\bar{t}hh \to t\bar{t}b\bar{b}b\bar{b}$ channel, arXiv:1410.1855; M. van Beekveld, W. Beenakker, S. Caron, R. Castelijn, M. Lanfermann, and A. Struebig, Higgs, di-Higgs and tri-Higgs production via SUSY processes at the LHC with 14 TeV, J. High Energy Phys. 05 (2015) 044; V. Martin-Lozano, J. M. Moreno, and C. B. Park, Resonant Higgs boson pair production in the $hh \to b\bar{b}WW \to b\bar{b}\ell^+\nu\ell^-\bar{\nu}$ decay channel, J. High Energy Phys. 08 (2015) 004; Q. Li, Z. Li, Q. S. Yan, and X. Zhao, Probe Higgs boson pair production via the $3\ell 2j$ + missing E_T mode, Phys. Rev. D **92**, 014015 (2015); N. Liu, Y. Zhang, J. Han, and B. Yang, Enhancing $t\bar{t}hh$ production through CP-violating top-Higgs interaction at the LHC, ILC and a 100 TeV collider, J. High Energy Phys. 09 (2015) 008.

[4] J. F. Gunion and H. E. Haber, Two-body decays of neutralinos and charginos, Phys. Rev. D **37**, 2515 (1988); S. Jung, Resolving the existence of Higgsinos in the LHC inverse problem, J. High Energy Phys. 06 (2014) 111.

[5] L. Basso, A. Belyaev, S. Moretti, and C. H. Shepherd-Themistocleous, Phenomenology of the minimal $B-L$ extension of the standard model: Z' and neutrinos, Phys. Rev. D **80**, 055030 (2009).

[6] G. Aad *et al.* (ATLAS Collaboration), Constraints on new phenomena via Higgs boson couplings and invisible decays with the ATLAS detector, J. High Energy Phys. 11 (2015) 206.

[7] G. Aad *et al.* (ATLAS Collaboration), Search for high-mass dilepton resonances in pp collisions at $\sqrt{s} = 8$ TeV with the ATLAS detector, Phys. Rev. D **90**, 052005 (2014).

[8] https://twiki.cern.ch/twiki/bin/view/LHCPhysics/CERNYellowReportPageAt14 TeV.

[9] K. Huitu, S. Khalil, H. Okada, and S. K. Rai, Signatures for Right-Handed Neutrinos at the Large Hadron Collider, Phys. Rev. Lett. **101**, 181802 (2008).

[10] A. Atre, T. Han, S. Pascoli, and B. Zhang, The search for heavy Majorana neutrinos, J. High Energy Phys. 05 (2009) 030.

[11] F. F. Deppisch, P. S. B. Dev, and A. Pilaftsis, Neutrinos and collider physics, New J. Phys. **17**, 075019 (2015).

[12] See Supplemental Material at http://link.aps.org/supplemental/10.1103/PhysRevLett.116.131801, which includes Refs. [13–21], for some detailed LHC analysis and introductions of models.

[13] Z. Kang, J. Li, T. Li, T. Liu, and J. Yang, Asymmetric sneutrino dark matter in the NMSSM with minimal inverse seesaw, arXiv:1102.5644; J. Guo, Z. Kang, T. Li, and Y. Liu, Higgs boson mass and complex sneutrino dark matter in the supersymmetric inverse seesaw models, J. High Energy Phys. 02 (2014) 080; H. An, P. S. Dev, Y. Cai, and R. N. Mohapatra, Sneutrino Dark Matter in Gauged Inverse Seesaw Models for Neutrinos, Phys. Rev. Lett. **108**, 081806 (2012).

[14] H. C. Cheng and I. Low, Little hierarchy, little higgses, and a little symmetry, J. High Energy Phys. 08 (2004) 061.

[15] L. W. Chen, R. Y. Zhang, W. G. Ma, W. H. Li, P. F. Duan, and L. Guo, Probing the littlest Higgs model with T parity using di-Higgs events through Z_H-pair production at the LHC in NLO QCD, Phys. Rev. D **90**, 054020 (2014).

[16] Z. Kang, J. Li, and T. Li, On naturalness of the MSSM and NMSSM, J. High Energy Phys. 11 (2012) 024.
[17] Z. Kang, Y. Liu, and G. Z. Ning, Highlights of supersymmetric hypercharge ± 1 triplets, J. High Energy Phys. 09 (2013) 091.
[18] T. J. LeCompte and S. P. Martin, Compressed supersymmetry after 1 fb^{-1} at the Large Hadron Collider, Phys. Rev. D **85**, 035023 (2012); Z. H. Yu, X. J. Bi, Q. S. Yan, and P. F. Yin, Detecting light stop pairs in coannihilation scenarios at the LHC, Phys. Rev. D **87**, 055007 (2013).
[19] J. Guo, Z. Kang, J. Li, and T. Li, Implications of Higgs sterility for the Higgs and stop sectors, arXiv:1308.3075.
[20] D. E. Ferreira de Lima, A. Papaefstathiou, and M. Spannowsky, Standard model Higgs boson pair production in the $(b\bar{b})(b\bar{b})$ final state, J. High Energy Phys. 08 (2014) 030.
[21] G. Aad *et al.* (ATLAS Collaboration), Search for Higgs boson pair production in the $b\bar{b}b\bar{b}$ final state from pp collisions at $\sqrt{s} = 8$ TeV with the ATLAS detector, Eur. Phys. J. C **75**, 412 (2015).
[22] M. J. Dolan, C. Englert, and M. Spannowsky, Higgs self-coupling measurements at the LHC, J. High Energy Phys. 10 (2012) 112.
[23] J. Grigo, J. Ho, K. Melnikov, and M. Steinhauser, On the Higgs boson pair production at the LHC, Nucl. Phys. **B875**, 1 (2013).
[24] V. Khachatryan *et al.* (CMS Collaboration), Search for resonant pair production of Higgs bosons decaying to two bottom quark-antiquark pairs in proton-proton collisions at 8 TeV, Phys. Lett. B **749**, 560 (2015).
[25] B. Cooper, N. Konstantinidis, L. Lambourne, and D. Wardrope, Boosted $hh \to b\bar{b}b\bar{b}$: A new topology in searches for TeV-scale resonances at the LHC, Phys. Rev. D **88**, 114005 (2013).
[26] M. Gouzevitch, A. Oliveira, J. Rojo, R. Rosenfeld, G. P. Salam, and V. Sanz, Scale-invariant resonance tagging in multijet events and new physics in Higgs pair production, J. High Energy Phys. 07 (2013) 148.
[27] Z. Kang, J. Li, T. Li, D. Liu, and J. Shu, Probing the CP-even Higgs sector via $H_3 \to H_2 H_1$ in the natural next-to-minimal supersymmetric standard model, Phys. Rev. D **88**, 015006 (2013).
[28] N. Chen, J. Li, Y. Liu, and Z. Liu, LHC searches for the CP-odd Higgs by the jet substructure analysis, Phys. Rev. D **91**, 075002 (2015).
[29] M. Backović, T. Flacke, J. H. Kim, and S. J. Lee, Boosted event topologies from TeV scale light quark composite partners, J. High Energy Phys. 04 (2015) 082.
[30] A. Chakraborty, D. K. Ghosh, S. Mondal, S. Poddar, and D. Sengupta, Probing the NMSSM via Higgs signatures from stop cascade decays at the LHC, Phys. Rev. D **91**, 115018 (2015).
[31] V. Khachatryan CMS Collaboration, CERN Technical Report No. CMS-PAS-SUS-13-022, 2014.
[32] G. Aad *et al.* (ATLAS Collaboration), Performance of missing transverse momentum reconstruction in proton-proton collisions at 7 TeV with ATLAS, Eur. Phys. J. C **72**, 1844 (2012).
[33] J. Alwall, M. Herquet, F. Maltoni, O. Mattelaer, and T. Stelzer, MadGraph 5: Going beyond, J. High Energy Phys. 06 (2011) 128.
[34] J. M. Campbell, R. K. Ellis, and D. L. Rainwater, Next-to-leading order QCD predictions for $W + 2$ jet and $Z + 2$ jet production at the CERN LHC, Phys. Rev. D **68**, 094021 (2003).
[35] V. Ahrens, A. Ferroglia, M. Neubert, B. D. Pecjak, and L. L. Yang, Precision predictions for the $t + t(\text{bar})$ production cross section at hadron colliders, Phys. Lett. B **703**, 135 (2011).
[36] A. Alloul, N. D. Christensen, C. Degrande, C. Duhr, and B. Fuks, FeynRules 2.0—A complete toolbox for tree-level phenomenology, Comput. Phys. Commun. **185**, 2250 (2014).
[37] L. Basso, S. Moretti, and G. M. Pruna, Theoretical constraints on the couplings of non-exotic minimal Z' bosons, J. High Energy Phys. 08 (2011) 122.
[38] T. Sjostrand, S. Mrenna, and P. Z. Skands, PYTHIA 6.4 physics and manual, J. High Energy Phys. 05 (2006) 026.
[39] J. de Favereau, C. Delaere, P. Demin, A. Giammanco, V. Lemaître, A. Mertens, and M. Selvaggi (DELPHES 3 Collaboration), DELPHES 3, A modular framework for fast simulation of a generic collider experiment, J. High Energy Phys. 02 (2014) 057.
[40] V. Khachatryan CMS Collaboration, CERN Technical Report No. CMS-PAS-BTV-13-001, 2013.
[41] M. Cacciari, G. P. Salam, and G. Soyez, FastJet user manual, Eur. Phys. J. C **72**, 1896 (2012).
[42] Y. L. Dokshitzer, G. D. Leder, S. Moretti, and B. R. Webber, Better jet clustering algorithms, J. High Energy Phys. 08 (1997) 001; M. Wobisch and T. Wengler, in *Proceedings of the Workshop on Monte Carlo Generators for HERA Physics, Hamburg, 1998-1999*, pp. 270–279.
[43] J. M. Butterworth, A. R. Davison, M. Rubin, and G. P. Salam, Jet Substructure as a New Higgs-Search Channel at the Large Hadron Collider, Phys. Rev. Lett. **100**, 242001 (2008).
[44] C. G. Lester and D. J. Summers, Measuring masses of semi-invisibly decaying particles pair produced at hadron colliders, Phys. Lett. B **463**, 99 (1999); A. Barr, C. Lester, and P. Stephens, m(T2): The truth behind the glamour, J. Phys. G **29**, 2343 (2003).
[45] Z. Kang, P. Ko, and J. Li, New avenues to heavy right-handed neutrinos with pair production at hadronic colliders, arXiv:1512.08373.
[46] N. Arkani-Hamed, L. J. Hall, H. Murayama, D. R. Smith, and N. Weiner, Small neutrino masses from supersymmetry breaking, Phys. Rev. D **64**, 115011 (2001); G. Belanger, M. Kakizaki, E. Park, S. Kraml, and A. Pukhov, Light mixed sneutrinos as thermal dark matter, J. Cosmol. Astropart. Phys. 11 (2010) 017; K.-Y. Choi and O. Seto, Light Dirac right-handed sneutrino dark matter, Phys. Rev. D **88**, 035005 (2013).
[47] N. Arkani-Hamed, A. G. Cohen, E. Katz, and A. E. Nelson, The Littlest Higgs, J. High Energy Phys. 07 (2002) 034.
[48] J. Hubisz and P. Meade, Phenomenology of the littlest Higgs with T-parity, Phys. Rev. D **71**, 035016 (2005).